Inorganic Chemistry

Article

pubs.acs.org/IC

Molten Salt Synthesis of a Mixed-Valent Lanthanide(III/IV) Oxychloride with an Unprecedented Sillen X_2^4 Structure: $Ce_{1.3}Nd_{0.7}O_3Cl$

Jean-François Vigier,[†,‡] Catherine Renard,*[,†] Natacha Henry,[†] Annabelle Laplace,[‡] and Francis Abraham[†]

[†]Unité de Catalyse et de Chimie du Solide, UCCS UMR CNRS 8181, ENSCL-USTL, Université Lille Nord de France, B.P. 90108, 59652 Villeneuve d'Ascq Cedex, France

[‡]CEA, Nuclear Energy Division, RadioChemistry & Processes Department, SCPS/LEPS, F-30207 Bagnols sur Cèze, France

Supporting Information

ABSTRACT: A new cerium neodymium oxychloride, $Ce_{1.3}Nd_{0.7}O_3Cl$, has been synthesized by precipitation in a $LiCl-CaCl_2$ molten salt by humid argon sparging. Chemical and structure characterization have been undertaken by powder X-ray diffraction, scanning electron microscopy, high-temperature X-ray diffraction, thermogravimetric analysis, and X-ray photoelectron scattering. This oxychloride crystallizes in space group $P4/nmm$, $a = 3.9848(3)$ Å and $c = 12.467(2)$ Å, in a new Sillen-type phase represented by the symbol X_2^4 where "quadruple" fluorite-type layers $[M_4O_6]$, containing Ce^{IV} in "inner" sublayers and both Ce^{III} and Nd^{III} in "outer" sublayers, alternate with double-halide ion sheets. The structure is also described as a stacking of LnOCl and fluorite-type blocks and constitutes the term $n = 2$ of a possible series $(MO_2)_n(NdOCl)_2$.

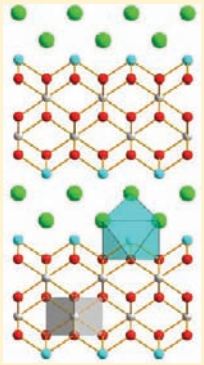

INTRODUCTION

Rare-earth (RE) oxychlorides have significant applications, in particular as phosphors for displays, up-conversion lasers, and other optoelectronic devices[1] and for bioimaging probes.[2] They are good candidates for solid electrolytes because of their high Cl^- ion conductivity associated with water insolubility.[3] They are also efficient solid catalysts for the synthesis of cyclic carbonates from supercritical CO_2[4] and methyl chloride from methane[5] and for the destruction of chlorinated hydrocarbons.[6] The concerned lanthanide(III) oxychlorides pertain to the LnOCl family. Different synthetic methods—pyrohydrolysis of NH_4LnCl_6 precursors, self-hydrolysis of $LnCl_3$ solutions, mechanochemical synthesis, surfactant-assisted solvothermal reaction, condensation of rare-earth chlorides and alkoxides in the presence of coordinating ligands—have been used to control the particle shape of the LnOCl compounds.[1a,2,7] On the other hand, oxidative precipitation of lanthanides from lanthanide chlorides in a molten salt is studied in the frame of nuclear fuel treatment by pyrochemical processes. Oxidative precipitation from $LnCl_3$ in an eutectic (LiCl–KCl) salt led to LnOCl oxychlorides for Ln = La, Pr, Nd, Sm, Eu, and Gd, to LnO_2 oxide for Ln = Ce and Pr, and to Y_2O_3.[8] Starting from a mixture of lanthanide chlorides led to a mixture of lanthanide oxychlorides or a mixture of lanthanide oxychloride and lanthanide oxide.[8d] During the precipitation study from mixtures of $CeCl_3$ and $NdCl_3$ in a $LiCl-CaCl_2$ salt using a modified oxidizing method, a new mixed Ce–Nd oxychloride containing both Ce^{III} and Ce^{IV} has been isolated and is described in this paper.

EXPERIMENTAL SECTION

The oxychloride $Ce_{1.3}Nd_{0.7}O_3Cl$ is synthesized in a molten salt, by precipitation of cerium and neodymium under wet argon. The experimental device used for precipitation is schematized in Figure 1. A high-form alumina crucible containing the salts is in a quartz reactor, placed in a vertical tubular oven. Argon is humidified by passing through a gas-washing bottle containing distilled water at 20 °C. The wet gas is fed into the reactor by an alumina tube. The output gases are neutralized by sparging in soda solutions. The chloride salts are a mixture of $LiCl-CaCl_2$ in a molar proportion of 30:70, and the melting temperature is 680 °C.[9] The reactants are $NdCl_3{\cdot}6H_2O$ and $CeCl_3{\cdot}7H_2O$ in an equimolar proportion. The masses are calculated to have 20 g of an anhydrous mixture, containing 10 wt % of lanthanides. The chlorides are blended in a mortar and put in the crucible, which is introduced in the quartz reactor. The salts are then dehydrated in situ. The reactor is purged with argon before heating at 150 °C for 6 h under a vacuum and 12 h under dry argon. Then the temperature is raised to 705 °C (2 °C/min). The alumina bubbling tube is then immersed in the molten salt. The dry argon sparging is maintained for 1 h, and bubbling with wet gas continues for 3 h. The oven is then switched off, the alumina tube is removed from the molten salt, and dry argon replaces wet argon while cooling to room temperature. The salt mixture containing the precipitate is dissolved in distilled water. The precipitate is filtered and dried in a dry oven at 100 °C. In a second step, the precipitate is washed with a dilute hydrochloric acid solution. The resulting powder is filtered, rinsed with distilled water, and dried at 100 °C. A fraction of the washed precipitate was heated at 1250 °C for 24 h under air.

Received: January 10, 2012
Published: March 19, 2012

dx.doi.org/10.1021/ic3000558 | Inorg. Chem. 2012, 51, 4352–4358

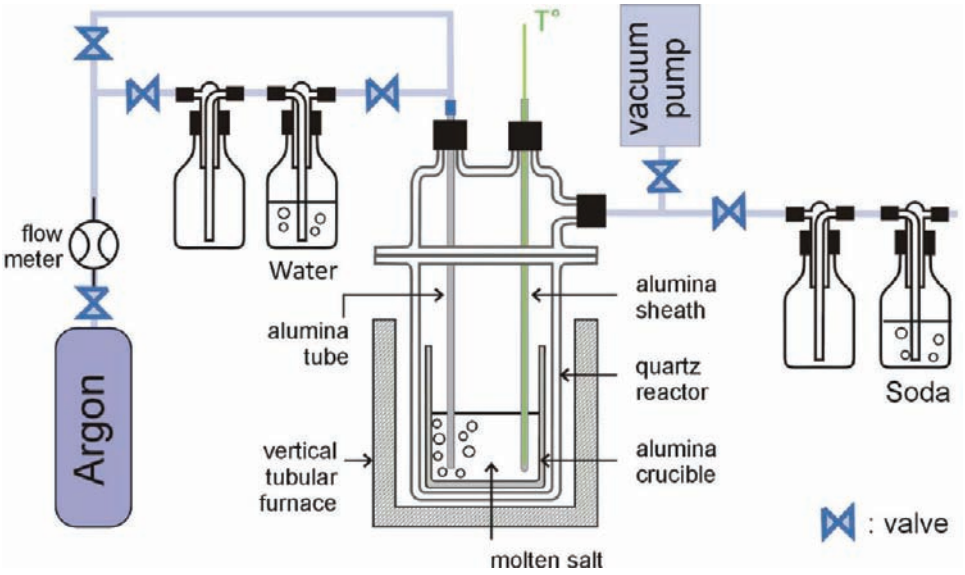

Figure 1. Experimental device for precipitation of oxychlorides or oxides in a molten salt by humid argon sparging.

The powder was observed on a Hitachi S4700 microscope equipped with a Bruker Quantax 400 EDS system, and the chemical composition was quantified by energy-dispersive spectrometry (EDS).

The precipitate, acid-washed powder, and sintered powder were analyzed by powder X-ray diffraction (XRD) on a Huber Guinier image plate G670 diffractometer for phase identification of the precipitate and on a D8 Advance Bruker diffractometer for phase identification and refinement of the unit-cell parameters (with JANA2006[10]) of the other samples. The crystal structure of $(Nd,Ce)_2O_3Cl$ was solved from powder XRD data on the acid-washed precipitate. Because of a high preferential orientation of the crystallites and the low quantity of powder, the sample was prepared by dusting the ground powder on an oriented silicon crystal sample holder. The XRD pattern was measured on a D8 Advance A25 Bruker diffractometer, with a lynxEye detector. The crystal structure was determined by an ab initio method using *EXPO*[11] and refined with *JANA2006*.[10] A surface roughness correction was applied using the Pitschke–Hermann–Matter model,[12] in accordance with the sample preparation. The sample contains $Ce_{0.8}Nd_{0.2}O_{1.9}$; this oxide was introduced in the refinement, but only the cell and peak profile parameters were refined. The diffraction measurement parameters and refinement results are summarized in Table 1; the calculated and measured XRD patterns are compared in Figure 2.

Thermal analyses were performed on a Setsys evolution thermogravimetric analyzer from Setaram, in a temperature range from 100 to 1300 °C (heating speed 5 °C/min), under air. The high-temperature XRD (HTXRD) diagrams were done on a D8 Advance Bruker diffractometer equipped with a Vantec detector and with a HTK 1200N Anton Paar high-temperature chamber, from 50 to 1100 °C, every 50 °C, under air.

X-ray photoelectron scattering (XPS) analyses were performed using a Kratos Analytical AXIS UltraDLD spectrometer. A monochromatized aluminum source (Al Kα = 1486.6 eV) was used for excitation. The X-ray beam diameter was around 1 mm. The analyzer was operated in a constant pass energy of 40 eV using an analysis area of approximately 700 μm × 300 μm. Charge compensation was applied to compensate for the charging effect occurring during analysis. The adventitious C 1s (285.0 eV) binding energy (BE) was used as an internal reference. The spectrometer BE scale was initially calibrated against the Ag 3d5/2 (368.2 eV) level. The pressure was in the 10^{-10} Torr range during the experiments. Quantification and simulation of the experimental photopeaks was carried out using *CasaXPS* software.

Table 1. Crystal Data and Structure Refinement Parameters for $Ce_{1.3}Nd_{0.7}O_3Cl$

diffractometer	D8 Bruker Advance
angular range/step (2θ, deg)	5–120°/0.019°
measurement temp (°C)	25
radiation	Cu Kα
no. of points	5910
total no. of refined param	28
no. of refined crystallographic param	11(3)
profile function	pseudo-Voigt
background function	manual background combined with eight Legendre polynoms
unit-cell param	a = 3.9848(2)
	c = 12.4670(12)
unit-cell volume	189.12(2)
space group	$P4/nmm$
formula units, Z	2
R_{obs} (wR_{obs})	0.0354 (0.0472)
R_p	0.0395
wR_p	0.0557

RESULTS AND DISCUSSION

Analysis of the Precipitate. The precipitate was first identified by powder XRD (Figure 3), it contains the new oxychloride $Ce_{1.3}Nd_{0.7}O_3Cl$, lanthanide oxychloride $Ce_{0.4}Nd_{0.6}OCl$ (majority compound), and $Ce_{0.8}Nd_{0.2}O_{1.9}$ (minority compound). The composition of the last compound was deduced from the refined cell parameter [a = 5.442(5)Å] compared to the $Ce_{1-x}Nd_xO_{2-0.5x}$ ones.[13] There is no bibliographic data on the $Ce_{1-x}Nd_xOCl$ solid solution. However, the study of $La_{1-x}RE_xOCl$ (RE = Gd and Y)[14] has shown that the cell parameter evolution obeys Vegard's law. CeOCl[15] and NdOCl,[16] like most of the lanthanide oxychlorides LnOCl,[17] crystallize in the PbClF structural type. So, when a linear evolution of the cell parameters of $Ce_{1-x}Nd_xOCl$ as a function of x is supposed and using the refined unit-cell parameters [a = 3.893(1) Å; c = 12.477(8) Å], the calculated formula is $Ce_{0.4}Nd_{0.6}OCl$. This oxychloride is soluble in diluted acid so the precipitate was washed with 0.1 M hydrochloric acid to eliminate this phase and facilitate the study of the new

dx.doi.org/10.1021/ic3000558 | *Inorg. Chem.* 2012, 51, 4352–4358

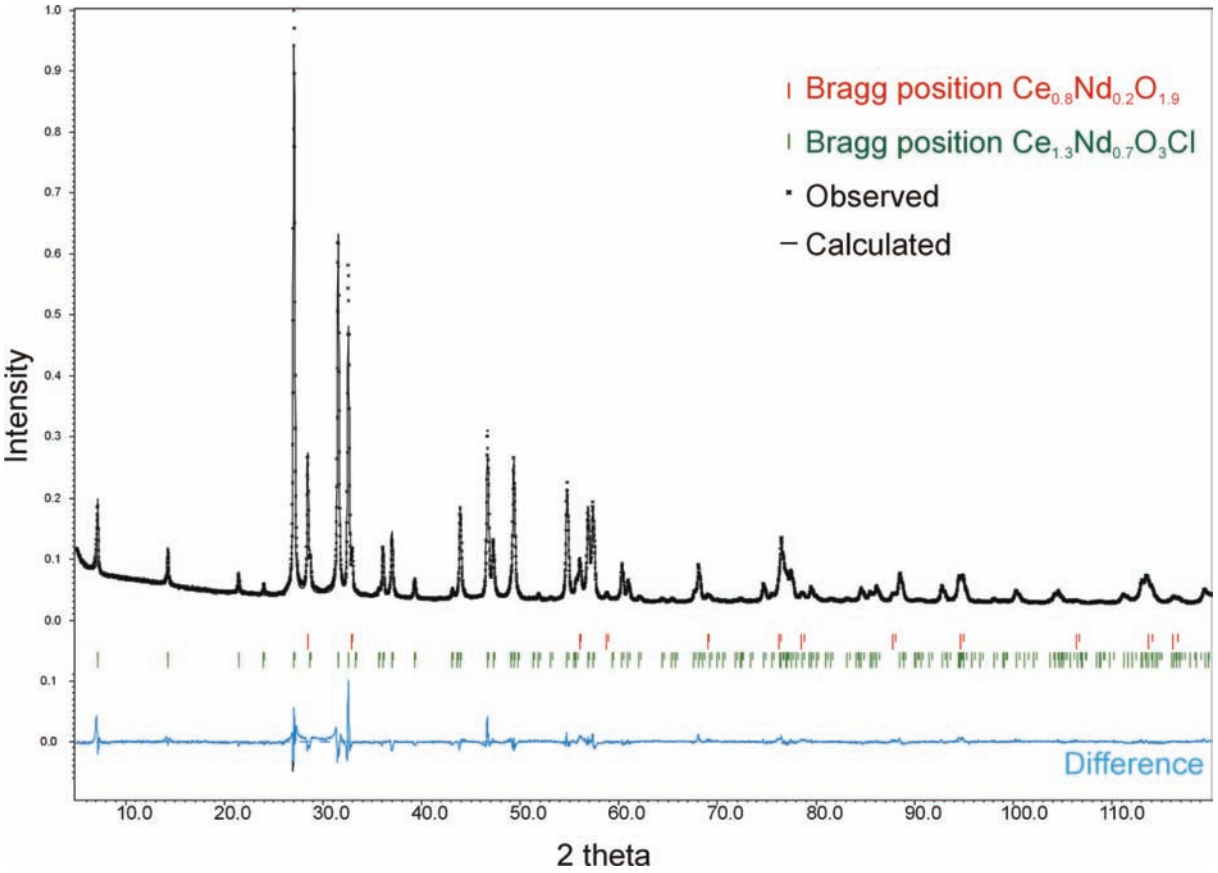

Figure 2. Observed and calculated XRD patterns of $Ce_{1.3}Nd_{0.7}O_3Cl$.

oxychloride. The $Ce_{1.3}Nd_{0.7}O_3Cl$ crystals are square plates (Figure 4); the larger crystals ($20 \times 20 \times 1$ μm^3) are too small for a X-ray data collection. The structure was therefore determined from powder XRD data.

Crystal Structure Description. $Ce_{1.3}Nd_{0.7}O_3Cl$ crystallizes in a tetragonal cell with $a = 3.9848(3)$ Å and $c = 12.467(2)$ Å; the structure was refined in the space group $P4/nmm$. The structure refinement parameters are reported in Table 1, and the refined atomic parameters in Table 2. The principal interatomic distances and angles are given in Table 3 and compared to those of LnOCl (Ln = Ce[15] and Nd[16]) and CeO_2. Nd1 and Ce1 share a 2c site with an occupancy (0.7Nd, 0.3Ce) fixed at the value deduced from the analyses discussed below.

$Ce_{1.3}Nd_{0.7}O_3Cl$ can be considered as a new member of the Sillen structural family. The first members of the Sillen series, BiOCl and LnOCl, contain double bismuth-based fluorite-type layers $[Bi_2O_2]$, which are, in fact, formed by a sheet of coplanar O with a sheet of Bi atoms on each side and single $[X_1]$, double $[X_2]$, or triple $[M'_xX_3]$ halide ion sheets stacked in the [001] direction of the "ideal" tetragonal cell, giving compounds denoted X_n (n for the number of halide ion layers) such as $MBiO_2Cl$ (M = alkaline-earth, Pb, and Cd) denoted X_1 (Figure 5a), BiOCl (X_2; Figure 5b), and $(M,Bi)_2M'_xO_2Cl_3$ (X_3), such as, for example, $Ca_{0.75}(Ca_{0.5}Bi_{1.5})O_2Cl_3$.[18] The lanthanide oxychlorides LnOCl are related to the X_2 series. Many intergrowths between these terms, such as $X_1 \times 2$ or $X_2 \times 3$, have been reported. The existence of triple fluorite-type layers $[M_3O_4]$ in, for example, Bi_3O_4Cl[19] and Bi_2LaO_4Cl[20] (Figure 5c), required one to extend the Sillen nomenclature to two indices X^n_m, where n is the number of cations in the fluorite-related layer and m the number in separating halide ion sheets;[21] for example, the symbol of the structure of Bi_3O_4Cl is X^3_1. In $Ce_{1.3}Nd_{0.7}O_3Cl$, "quadruple" fluorite-type layers $[M_4O_6]$ alternate with double halide ion sheets, giving, to our knowledge, a new Sillen-type phase X^4_2 (Figure 5d). In the "quadruple" fluorite-type layer, the two "inner" sublayers contain Ce^{4+} ions (Ce2 in a 2c site) coordinated by four O1 atoms at 2.34(2) Å and four O2 atoms at 2.362(4) Å (Figure 6a), forming distorted $Ce2O_8$ cubes that are connected by edges to form two cube-height fluorine-type layers $Ce2O_3$. The trivalent lanthanides Nd1 and Ce1 that constitute the "outer" sublayers are hanged to the O1 atoms to form square pyramids $Ln1O1_4$ (Ln = Nd and Ce). In this description, the Ln1 coordination polyhedron is open. In fact, the $Ln1^{3+}$ ions are surrounded by four Cl1 atoms at 3.072(9) Å to form, with the O1 atoms at 2.34(2) Å, a square antiprism as in the simplest Sillen phases. The coordination polyhedron is completed by one Cl ion at a longer distance, 3.24(2) Å, to give a capped square antiprism (Figure 6b). If the Ln1−Cl bonds are taken into account, another interesting description of the structure of $Ce_{1.3}Nd_{0.7}O_3Cl$ can be constructed using the polyhedral assemblage. The $(Nd,Ce)O_4Cl_4$ square antiprisms share the Cl_2O triangular faces and create layers parallel to (001). The Cl atoms of a square antiprism are the capping Cl atoms of four square antiprisms of an adjacent layer, creating $(Nd,Ce)O_2Cl$ double layers. The $(Nd,Ce)O_2Cl$ and $Ce2O_3$ double fluorite-type layers (Figure 7a) alternate in the [001] direction and are shared by their outer O atoms to form a three-dimensional arrangement. In NdOCl, the NdO_2Cl double layers are directly connected together by sharing the outer O atoms (Figure 7b). The $Ce_{1.3}Nd_{0.7}O_3Cl$ structure can be considered as an intergrowth between NdOCl and CeO_2 structural blocks. The

dx.doi.org/10.1021/ic3000558 | Inorg. Chem. 2012, 51, 4352−4358

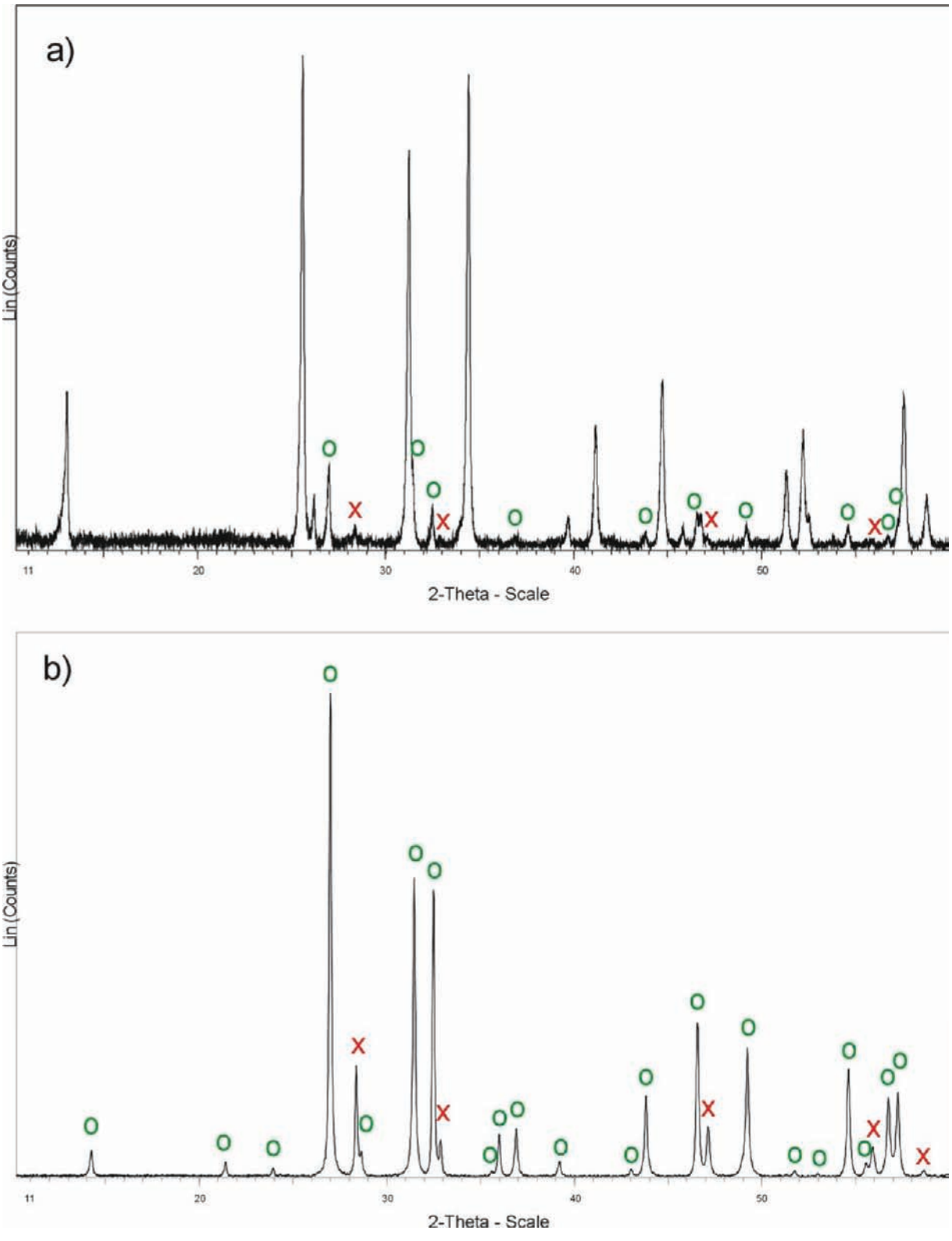

Figure 3. (a) Powder XRD diagram of the precipitate containing, lanthanide oxychloride $Ce_{0.4}Nd_{0.6}OCl$ (unmarked), $Ce_{0.8}Nd_{0.2}O_{1.9}$ (×) and the new oxychloride (○). (b) X-ray pattern of the acid washed powder, $Ce_{0.4}Nd_{0.6}OCl$ disappears after washing with a 0.1 M HCl solution.

a cell parameter of $Ce_{1.3}Nd_{0.7}O_3Cl$, a = 3.8948(3) Å, is intermediate between that of NdOCl [a = 4.0249(2) Å] and that of CeO_2 ($a/\sqrt{2}$ = 3.8263 Å). So, the $Ce2O_8$ cubes are stretched in the (001) plane compared to the CeO_8 fluorite cubes, giving a thickness of the fluorite-type layer reduced from 5.412(1) Å in CeO_2 to 5.26(6) Å in $Ce_{1.3}Nd_{0.7}O_3Cl$. In the opposite direction, the decrease of the *a* parameter from NdOCl to $Ce_{1.3}Nd_{0.7}O_3Cl$ causes the stretching of the LnO_4Cl_5 polyhedra in the [001] direction from 4.268(8) to 4.54(6) Å and a large increase of the thickness of the $(Nd,Ce)O_2Cl$ double layers from 6.7837(5) to 7.21(1) Å. It is noticeable that, in the LnO_4Cl_5 polyhedra, the Nd−Cl distance with the

dx.doi.org/10.1021/ic3000558 | *Inorg. Chem.* 2012, 51, 4352−4358

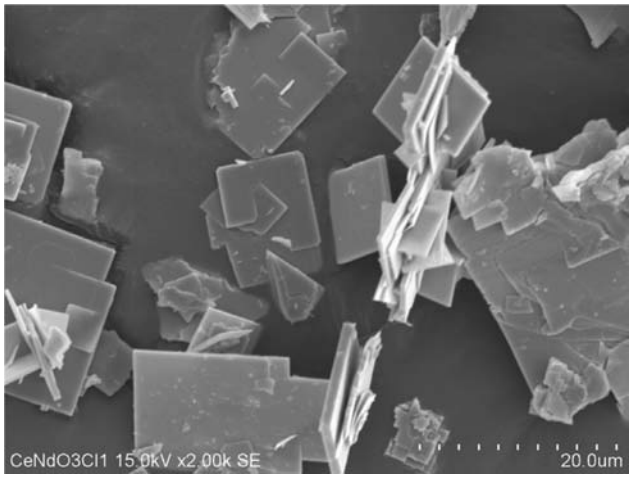

Figure 4. Scanning electron microscopy image of $Ce_{1.3}Nd_{0.7}O_3Cl$ crystals.

Table 2. Atomic Coordinates and Isotropic Displacement Parameters (A^2) for $Ce_{1.3}Nd_{0.7}O_3Cl$

atom	occupancy	*x*	*y*	*z*	*U*
Nd1	0.7	$^1/_2$	0	0.6845(4)	0.014(3)
Ce1	0.3	$^1/_2$	0	0.6845	0.014
Ce2		0	$^1/_2$	0.8928(5)	0.008(2)
Cl		0	$^1/_2$	0.575(2)	0.019(7)
O1		$^1/_2$	$^1/_2$	0.789(3)	0.022(9)
O2		$^1/_2$	$^1/_2$	0	0.022

capping Cl atom [3.082(8) Å] is shorter than the four others in NdOCl, when it is longer in $Ce_{1.3}Nd_{0.7}O_3Cl$. This is accompanied by a decrease in the O1−Ln−O1 and Cl−Ln−Cl angles and a lengthening of the Ln−Cl bond parallel to *c* compared to LnOCl (Ln = Nd or Ce) ones (Table 3). As a consequence, the *c* parameter, 12.467(2) Å, is slightly higher than the sum of the oxide and oxychloride *c* parameters: 5.4124(1) + 6.7837(5) = 12.1961(6) Å. In fact, the introduction of the more rigid fluorite-type layers leads to a strong deformation of the flexible lanthanide oxychloride arrangement.

$Ce_{1.3}Nd_{0.7}O_3Cl$ is the first example of a Sillen-type phase with a quadruple fluorite-type layer and with a tetravalent metal. Lanthanide(III)−metal(IV) compounds with the same formula $LnM^{IV}O_3Cl$ have been reported for M = Ti and Ln = Sm−Lu, $LnTiO_3Cl$.[22] In their structures, the smaller Ti^{IV} ion is

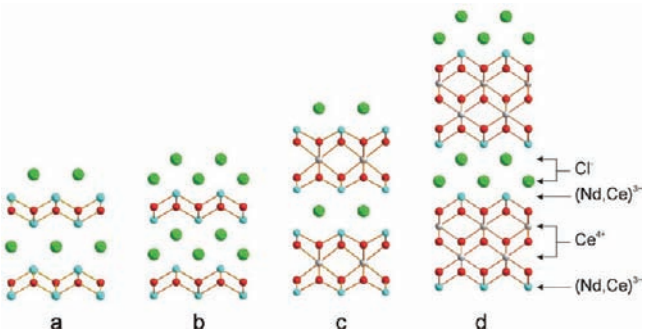

Figure 5. Intergrowth of fluorite-type layers $[M_2O_2]$ and single or double halide ion sheets in the first members X_1 (a) and X_2 (b) of the Sillen series. In, for example, Bi_2LaO_4Cl, triple fluorite-type layers $[M_3O_4]$ alternate with single Cl^- sheets, type X_1^3 (c). In $Ce_{1.3}Nd_{0.7}O_3Cl$, quadruple fluorite-type layers $[M_3O_4]$ alternate with double Cl^- sheets, novel type X_2^4 (d).

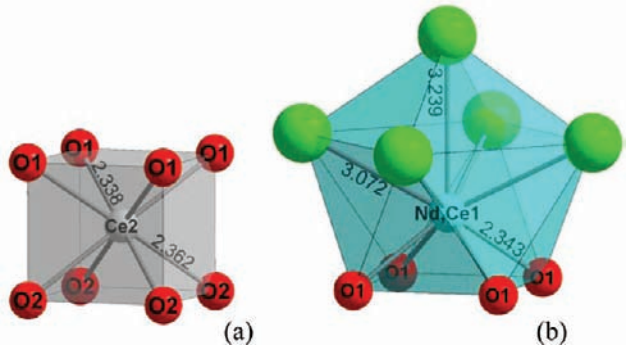

Figure 6. Cation coordination polyhedra in $Ce_{1.3}Nd_{0.7}O_3Cl$: Ce2 (a); Nd1 and Ce1 (b).

in a distorted octahedral environment and the layers are no longer of the fluorite type.

Thermal Behavior. The powder HTXRD diagrams show that oxychloride starts to transform into oxide at 500 °C and is completely converted into $Ce_{1-x}Nd_xO_{2-0.5x}$ at 900 °C (Figure 8). This conversion is accompanied by a two-step weight loss observed by thermogravimetric analysis (TGA), which indicates an end of decomposition at 980 °C (Figure 9). This difference is probably due to the heating speed difference. The temperature of decomposition is lower than that of NdOCl.[23] The XRD pattern of the sintered sample contains two solid solutions of cerium neodymium oxide: the as-precipitated $Ce_{0.8}Nd_{0.2}O_{1.9}$ and $Ce_{0.65}Nd_{0.35}O_{1.825}$ resulting from decom-

Table 3. Main Angles (deg) and Distances (Å) in $Ce_{1.3}Nd_{0.7}O_3Cl$, Compared to LnOCl (Ln = Nd or Ce) and CeO_2 Ones

$Ce_{1.3}Nd_{0.7}O_3Cl$		NdOCl		CeOCl		CeO_2	
Nd−Ce1−O1	2.35(2) (4×)	Nd−O	2.336 (4×)	Ce−O	2.364 (4×)		
Nd−Ce1−Cl	3.072(9) (4×)	Nd−Cl	3.141 (4×)	Ce−Cl	3.180 (4×)		
	3.24(2)		3.082		3.103		
Ce2−O1	2.34(2) (4×)					Ce−O	2.343 (8×)
Ce2−O2	2.362(3) (4×)						
O1−Nd−Ce1−O1	72.0	O−Nd−O	75.1	O−Ce−O	75.2		
Cl−Nd−Ce1-Cl	78.7	Cl−Nd−Cl	79.7	Cl−Ce−Cl	79.8		
Cl−Nd−Ce1−O1	73.7	Cl−Nd−O	70.3	Cl−Ce−O	70.1		
O1−Ce2−O1	72.2					O−Ce−O	70.53
O2−Ce2−O2	71.3						
O1−Ce2−O2	68.0						

dx.doi.org/10.1021/ic3000558 | *Inorg. Chem.* 2012, 51, 4352−4358

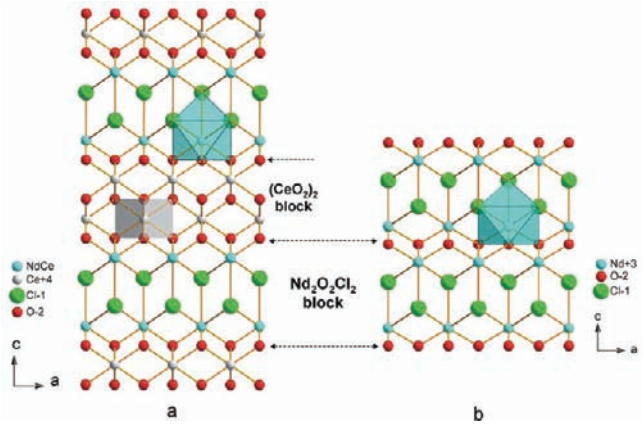

Figure 7. Structures of (a) $Ce_{1.3}Nd_{0.7}O_3Cl$ and (b) NdOCl.

position of $Ce_{1.3}Nd_{0.7}O_3Cl$. The composition of this oxide was deduced from the refined cell parameter [a = 5.47186(7)Å] compared to the $Ce_{1-x}Nd_xO_{2-0.5x}$ ones. This composition is in good agreement with EDS analysis on oxychloride crystals, which gave Ce:Nd = 68:32. The composition of the studied oxychoride is thus $Ce_{1.3}Nd_{0.7}O_3Cl$, the composition used in the structural study. According to this formula, the oxidation state of the cerium is mixed-valent III+/IV+ with an average 3.77. XPS analysis (Figure 10) of the washed precipitate confirms the presence of trivalent and tetravalent cerium. The Ce 3d spectrum is a complex superposition of Ce^{3+} and Ce^{4+} peaks. The spectrum displays u′ and v′ peaks, characteristic of trivalent cerium. The method described by Shyu et al.[24] was used to quantify the Ce^{4+} ratio. The u‴ peak is only related to tetravalent cerium; the Ce^{4+} ratio can be calculated with the u‴ area percentage in the Ce 3d region. The washed precipitate contains 85(8)% Ce^{4+}. Taking into account the presence of a

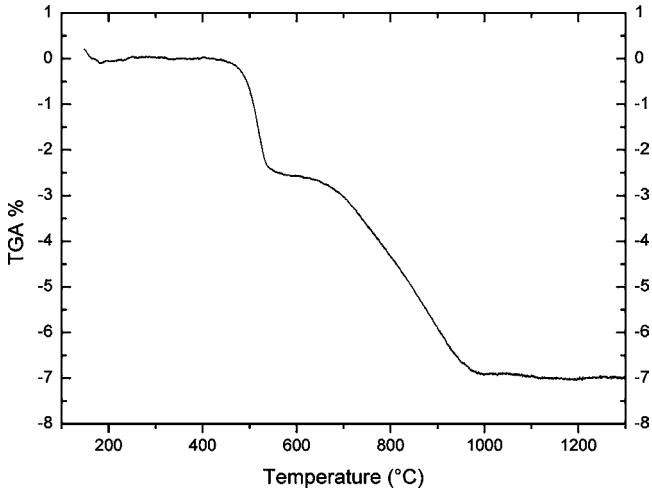

Figure 9. TGA of the washed precipitate.

cerium−neodymium oxide solid solution, this result corroborates the proposed composition. The oxychloride formula can be written as $Ce^{IV}(Ce^{III}_{0.3}Nd^{III}_{0.7})O_3Cl$.

CONCLUSION

$Ce_{1.3}Nd_{0.7}O_3Cl$ is the first mixed-valent cerium oxyhalide reported until now. Several works[25] have been published on the precipitation of lanthanide in a molten salt. The lanthanide compounds precipitate by oxygen sparging, in the form of LnOCl for various lanthanides including neodymium, or oxides, as is the case of cerium. The previous precipitation experiments on cerium systematically lead to cerium dioxide. In our work, water, brought into the molten salt via argon bubbling, is less oxidant than oxygen. This allowed the synthesis of a mixed-valent oxychloride $Ce_{1-x}Nd_xOCl$, containing Ce^{III}, and the

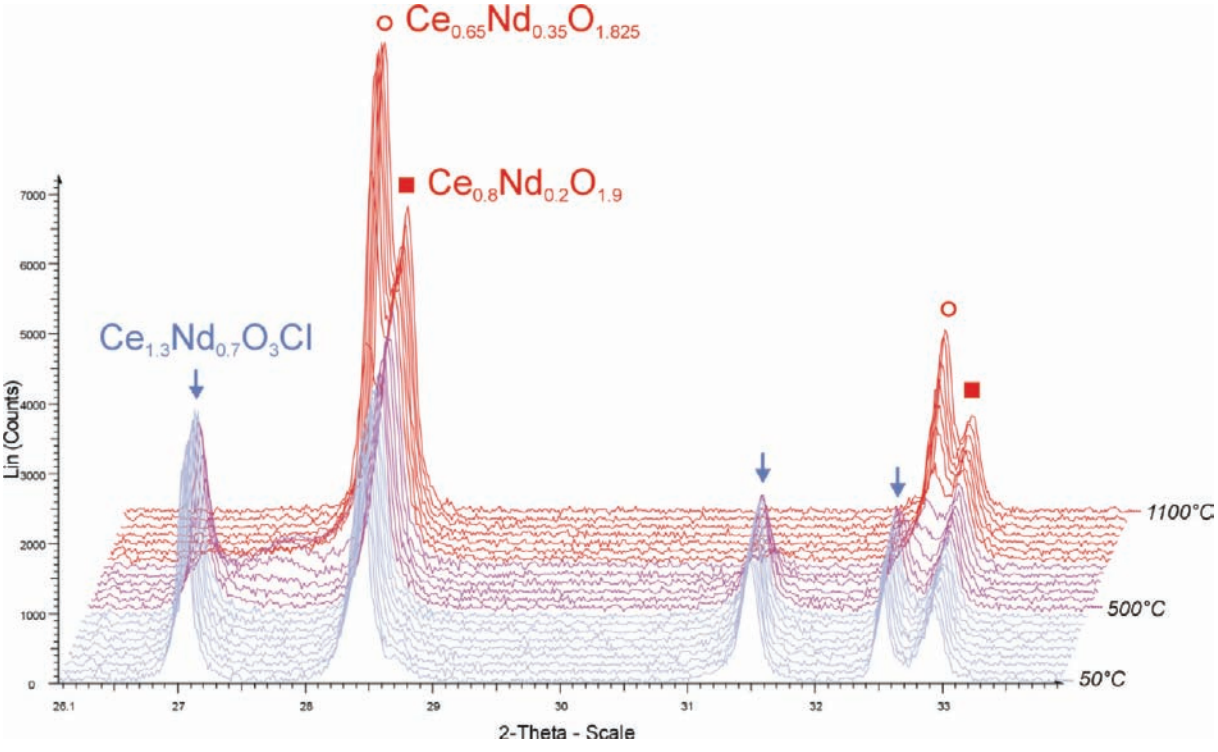

Figure 8. HTXRD patterns of the washed precipitate.

dx.doi.org/10.1021/ic3000558 | Inorg. Chem. 2012, 51, 4352−4358

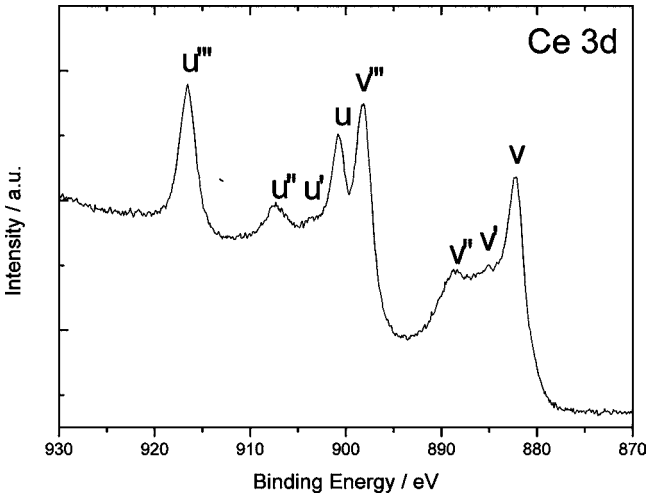

Figure 10. Ce 3d core-level XPS spectrum of the washed precipitate.

mixed-valent cerium oxychloride $Ce_{1.3}Nd_{0.7}O_3Cl$, which crystallizes in a new structure. The use of wet inert gas sparging in molten salts opens the way to the synthesis of new oxyhalides. The introduction of a quadruple fluorite-type layer in the Sillen-type family suggests the possibility of preparing the terms X_1^4 and X_3^4. The discovery of this compound with stacking of LnO_2Cl and fluorite-type blocks containing metal(IV) suggests an extensive new family with various thicknesses of the two blocks, $(M^{IV}O_2)_n[(LnOCl)_2]_{n'}$, $Ce_{1.3}Nd_{0.7}O_3Cl$, corresponding to $n = 2$ and $n' = 1$. The synthesis of such compounds is plane with other tetravalent metals.

■ ASSOCIATED CONTENT

Supporting Information

X-ray crystallographic data in CIF format. This material is available free of charge via the Internet at http://pubs.acs.org.

■ AUTHOR INFORMATION

Corresponding Author

*E-mail: catherine.renard@ensc-lille.fr.

Notes

The authors declare no competing financial interest.

■ ACKNOWLEDGMENTS

This work was partially supported by the "Groupement National de Recherche", PARIS. Anne-Sophie Mamède is greatly acknowledged for XPS experiments.

■ REFERENCES

(1) (a) Rambabu, U.; Annapurna, K.; Balaji, T.; Buddhudu, S. *Mater. Lett.* **1995**, *23*, 143−146. (b) Rambabu, U.; Mathur, A.; Buddhudu, S. *Mater. Chem. Phys.* **1999**, *61*, 156−162. (c) Holsa, J.; Lamminmaki, R.-J.; Lastusaari, M.; Porcher, P. *J. Alloys Compd.* **2001**, *323*−*324*, 811−815. (d) Li, G.; Li, C.; Zhang, C.; Cheng, Z.; Quan, Z.; Peng, C.; Lin, J. *J. Mater. Chem.* **2009**, *19*, 8936−8943.

(2) Konichi, T.; Shimizu, M.; Kameyama, Y.; Soga, K. *J. Mater. Sci.: Mater. Electron.* **2007**, *18*, S183−S186.

(3) (a) Okamoto, K.; Imanaka, N.; Adachi, G.-Y. *Solid State Ionics* **2002**, *154*−*155*, 577−580. (b) Imanaka, N.; Okamoto, K.; Adachi, G.-Y. *Angew. Chem.. Int. Ed.* **2002**, *41*, 3890−3892.

(4) Yasuda, H.; He, L.-N.; Sakakura, T. *J. Catal.* **2002**, *209*, 547−550.

(5) Podkolzin, S. G.; Stangland, E. E.; Jones, M. E.; Peringer, E.; Lercher, J. A. *J. Am. Chem. Soc.* **2007**, *129*, 2569−2576.

(6) Van der Avert, P.; Weckhuysen, B. M. *Angew. Chem., Int. Ed.* **2002**, *41*, 4730−4731.

(7) (a) Garcia, E.; Corbett, J. D.; Ford, J. E.; Vary, W. J. *Inorg. Chem.* **1985**, *24*, 494−498. (b) Lee, J.; Zhang, Q.; Saito, F. *J. Solid State Chem.* **2001**, *160*, 469−473. (c) Lee, S.-S.; Park, H.-I.; Joh, C.-H.; Byeon, S.-H. *J. Solid State Chem.* **2007**, *180*, 3529−3534. (d) Kort, K. R.; Banerjee, S. *Inorg. Chem.* **2011**, *50*, 5539−5544.

(8) (a) Cho, Y.-J.; Yang, H.-C.; Eun, H.-C.; Kim, E.-H.; Kim, I.-T. *J. Nucl. Sci. Technol.* **2006**, *43*, 1280−1286. (b) Eun, H.-C.; Cho, Y.-J.; Yang, H.-C.; Park, H. S.; Kim, E.-H.; Kim, I.-T. *J. Radioanal. Nucl. Chem.* **2007**, *274*, 621−624. (c) ChoY.-Z.YangH.-C.EunH.-C.KimE.-H.ParkH.-S.KimI.-T.*Proceedings of Global 2007: Advanced Nuclear Fuel Cycles and Systems*, Boise, ID, Sept 2007; Vols. *9*−*13*, pp 1416−1419. (d) Cho, Y.-Z.; Park, G.-H.; Yang, H.-C.; Han, D.-S.; Lee, H.-S.; Kim, I.-T. *J. Nucl. Sci. Technol.* **2009**, *46*, 1004−1014.

(9) Mahendran, K. H.; Nagaraj, S.; Sridharan, R.; Gnanasekaran, T. *J. Alloys Compd.* **2001**, *325*, 78−83.

(10) Petricek, V.; Dusek, M.; Palatinus, L. *Jana2006. Structure Determination Software Programs*; Institute of Physics: Praha, Czech Republic, 2006.

(11) Altomare, A.; Burla, M. C.; Camalli, M.; Carrozzini, B.; Cascarano, G. L.; Giacovazzo, C.; Guagliardi, A.; Moliterni, A. G. G.; Polidori, G.; Rizzi, R. *J. Appl. Crystallogr.* **1999**, *32*, 339−340.

(12) Pitschke, W.; Hermann, H.; Mattern, N. *Powder Diff.* **1993**, *8* (2), 74−83.

(13) Horlait, D.; Claparède, L.; Clavier, N.; Szenknect, S.; Dacheux, N.; Ravaux, J.; Podor, R. *Inorg. Chem.* **2011**, *50*, 7150−7161.

(14) Hölsä, J.; Kestiliä, E.; Kolski, K.; Rahila, H. *J. Alloys Compd.* **1995**, *225* (1−2), 193−197.

(15) Wolcyrz, M.; Kepinski, L. *J. Solid State Chem.* **1992**, *99* (2), 409−413.

(16) Meyer, G.; Schleid, T. *Z. Anorg. Allg. Chem.* **1986**, *533*, 181−185.

(17) (a) Garcia, E.; Corbett, J. D.; Ford, J. E.; Vary, W. *Inorg. Chem.* **1985**, *24* (4), 494−498. (b) Templeton, D. H.; Dauben, C. H. *J. Am. Chem. Soc.* **1953**, *75*, 6069−70.

(18) Sillen, L. G.; Gjoerling-Husberg, A. S. *Z. Anorg. Allg. Chem.* **1941**, *248*, 121−p134.

(19) Eggenweiler, U.; Keller, E.; Kraemer, V.; Meyer, C. A.; Ketterer, J. *Z. Kristallogr.-New Cryst. Struct.* **1998**, *213*, 695−695.

(20) Milne, C. J.; Lightfoot, P.; Jorgensen, J. D.; Short, S. *J. Mater. Chem.* **1995**, *5*, 1419−1421.

(21) Berdonosov, P. S.; Charkin, D. O.; Kusainova, A. M.; Hervoches, C. H.; Dolgikh, V. A.; Lightfoot, P. *Solid State Sci.* **2000**, *2*, 553−562.

(22) Huebner, N.; Fiedler, K.; Preuss, A.; Gruehn, R. *Z. Anorg. Allg. Chem.* **1993**, *619* (7), 1214−1220.

(23) Yang, H. C.; Cho, Y. J.; Eun, H. C.; Kim, E. H.; Kim, I. T. *Thermochim. Acta* **2007**, *460*, 53−59.

(24) Shyu, J. Z.; Otto, K.; Watkins, W. L. H.; Graham, G. W.; Belitz, R. K.; Gandhi, H. S. *J. Catal.* **1988**, *114*, 23−33.

(25) (a) Cho, Y.-J.; Yang, H.-C.; Eun, H.-C.; Kim, E.-H.; Kim, I.-T. *J. Nucl. Sci. Technol. (Tokyo, Jpn.)* **2006**, *43* (10), 1280−1286. (b) Cho, Y.-J.; Yang, H.-C.; Eun, H.-C.; Kim, E.-H.; Kim, J.-H. *J. Ind. Eng. Chem.* **2005**, *11* (5), 707−711. (c) Garcia, E.; Griego, W. J.; Owens, S. D.; Thorn, C. W.; Vigil, R. A. *Proc. Electrochem. Soc.* **1993**, *93-9* (Molten Salt Chemistry and Technology, 1993), 202−209.